Collision Energy Resolved Penning Ionization Electron Spectroscopy of Azines: Anisotropic Interaction of Azines with He*(2^3S) Atoms and Assignments of Ionic States

Naoki Kishimoto and Koichi Ohno*

Department of Chemistry, Graduate School of Science, Tohoku University, Aoba-ku, Sendai 980-8578, Japan

Received: March 14, 2000; In Final Form: May 2, 2000

Ionization of azines (*s*-triazine, pyridazine, pyrimidine, pyrazine, and pyridine) with He*(2^3S) metastable atoms was studied by (collision-energy/electron-energy-resolved) two-dimensional Penning ionization electron spectroscopy. Collision energy dependence of the partial ionization cross sections (CEDPICS), which reflects interaction potential energy between the molecule and He*(2^3S), showed anisotropic interaction around the molecules. Assignments of the Penning ionization electron spectra and ultraviolet photoelectron spectra were discussed on the basis of different behavior (positive or negative slope) of CEDPICS. Theoretically computed CEDPICS of *s*-triazine by classical trajectory calculations were found to be useful to confirm the assignment of the ionic states.

I. Introduction

To elucidate a chemical reaction, it is important to investigate dynamics of particles on the anisotropic interaction potential energy surface. A chemi-ionization process known as Penning ionization[1−4] is induced by collision of a reactant molecule M and a metastable atom A*, where A* has a larger excitation energy than the lowest ionization potential (IP) of M

$$M + A^* \rightarrow M^+ + A + e^- \quad (1)$$

Collision energy (E_c) dependence of total Penning ionization cross section $\sigma_T(E_c)$, which reflects interaction potentials between the colliding particles, has been measured by observing product ion intensity as functions of E_c of an A* atom.[5−12]

The electron exchange model[13] was proposed for the Penning ionization process. In this model, an electron in a molecular orbital (MO) of M is transferred to the inner-shell orbital of A* and the excited electron in A* is ejected. Penning ionization electron spectroscopy,[14] therefore, provides us information on the electron density distribution of the target MOs exposed outside the boundary surface of collision.[15] Then the state-resolved measurement of the collision energy dependence of partial ionization cross sections $\sigma_i(E_c)$ for the *i*th ionic state enables us to investigate anisotropic potential energy surface around the target molecule because the most effective direction for the collisional ionization is different depending upon the more or less localized electron distributions of the target MOs.

Coupled techniques including velocity (or collision energy) selection of He*(2^3S) metastable atoms and electron kinetic energy analysis[16] have been developed to yield (collision-energy/electron-energy-resolved) two-dimensional Penning ionization electron spectroscopy.[17] Collision energy dependence of the partial ionization cross sections (CEDPICS), which reflects anisotropic interaction between M and He*, has been observed for small simple molecules,[16,18] unsaturated hydrocarbons,[19] organic molecules including heteroatoms,[20] aromatic compounds (benzene,[19,21a] polycyclic aromatic hydrocarbons,[21b] five-membered heterocyclic compounds,[21c] and [2,2]-paracyclophane[21a]), and an organometallic compound.[22]

On the other hand, theoretical calculations of CEDPICS were limited to small molecules such as H_2[23] and N_2[24−26] because of the difficulty in potential energy surface and collision dynamics calculations. Recently, ionization of a polyatomic molecule, CH_3Cl, was studied[27] with Ne* beam and quasiclassical trajectory calculations within the assumption that ionization takes place only at the classical turning point. Classical trajectory calculations for N_2,[26] NCCN,[28] and CH_3CN[29] have been performed based on simplified models for potential energy surface and ionization width, accumulating ionization probability on the trajectories; the theoretical CEDPICS showed good agreement with experimental results.

In this study, we have measured CEDPICS of azines (*s*-triazine, pyridazine, pyrimidine, pyrazine, and pyridine) with the two-dimensional Penning ionization electron spectroscopy.[17] Anisotropic interaction potential around the molecule was investigated using ab initio molecular orbital calculation or a density functional theory (DFT), and assignments for the Penning ionization electron spectrum (PIES) of these molecules and the He I ultraviolet photoelectron spectrum (UPS) are discussed based on PIES band intensity and its change with respect to collision energies. For *s*-triazine, different behavior (positive or negative slope) of CEDPICS was obtained theoretically using trajectory calculation[26,29] of He* atoms on the three-dimensional potential energy surface, reflecting the anisotropic interaction around the molecule (attractive interaction around the nitrogen atoms and repulsive interaction around σ_{CH} bonds and out-of-plane direction). Assignments of the ionic states in UPS and PIES of *s*-triazine were confirmed by the theoretical CEDPICS.

II. Experimental Section

Metastable beam of He*(2^1S, 2^3S) were produced by a discharge nozzle source with a tantalum hollow cathode,[16,30] and the He*(2^1S) component was quenched by a water-cooled helium discharge lump. He I UPS were measured by using the He I resonance photons (584 Å, 21.22 eV) produced by a discharge in pure helium gas. The kinetic energy of ejected electrons was measured by a hemispherical electronic deflection type analyzer using an electron collection angle 90° to the

10.1021/jp000973l CCC: $19.00
Published on Web 07/08/2000

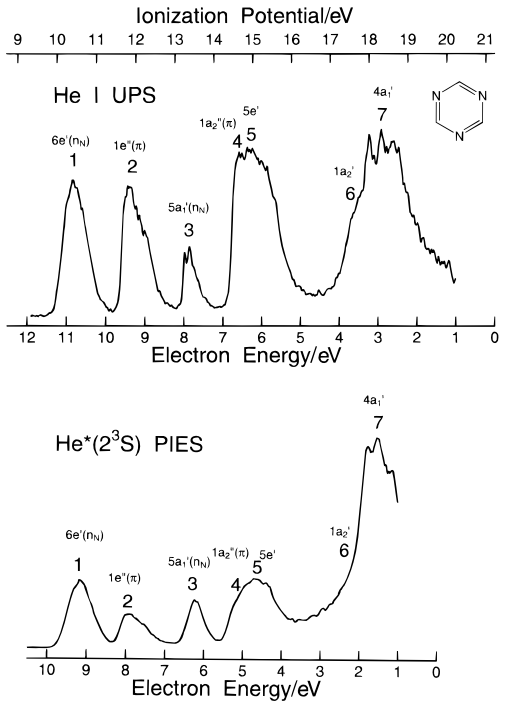

Figure 1. He I UPS and He*(2^3S) PIES of *s*-triazine.

incident He* or photon beam. We estimate the energy resolution of the electron energy analyzer to be 60 meV from the full width at half-maximum (fwhm) of the $Ar^+(^2P_{3/2})$ peak in the He I UPS. The transmission efficiency curve of the electron analyzer was determined by comparing our UPS data with those by Gardner and Samson[31] and Kimura et al.[32] The background pressure of the reaction chamber was on the order of 10^{-7} Torr.

For collision-energy-resolved measurements, we have measured two-dimensional spectra $I_e(E_e,t)$ as a function of electron kinetic energy E_e and time t utilizing two-dimensional measuring technique[17] and a time-of-flight (TOF) method with a mechanical chopper.[16,33] The He*(2^3S) metastable beam was introduced into the reaction cell located 504 mm downstream from the chopper disk. The resolution of the analyzer was lowered to 250 meV in order to obtain higher count rates. The observed two-dimensional spectra can lead to two-dimensional Penning ionization cross section normalized by the velocity distribution of the He*(2^3S) beam that was determined by monitoring secondary electrons emitted from an inserted stainless electron steel plate in the reaction cell.[16]

III. Calculations

To obtain electron density contour maps and schematic diagrams of MOs, ab initio self-consistent field (SCF) calculations were performed with 4-31G basis functions. The geometries of neutral target molecules were selected from literature for *s*-triazine,[34] pyrazine,[35] pyrimidine,[35] pyridazine,[36] and pyridine.[37] Schematic diagrams of MOs with circles and ellipses were used as in a previous study.[21c] In-plane p-type orbitals were shown by couples of ellipses. Out-of-plane components of p orbitals were shown by dashed circles. Valence s orbitals were shown by solid circles. Electron density contour maps were also used with thick solid curves indicating the repulsive molecular surface approximated by van der Waals radii.[38]

Interaction potential V was calculated on the basis of the well-known resemblance between He*(2^3S) and Li(2^2S); the shape of the total scattering cross section of He*(2^3S) by He, Ar, Kr is very similar to that of Li(2^2S),[39] and the location of the interaction potential well and its depth are very similar for He*-

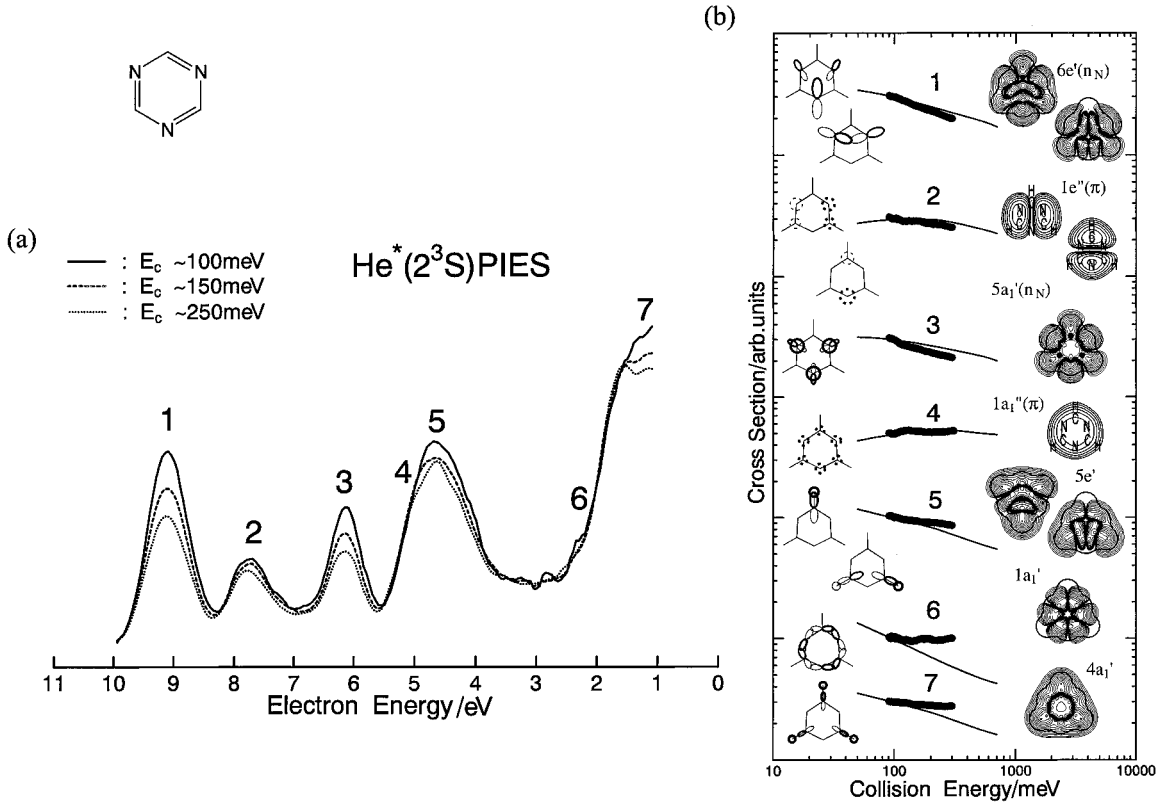

Figure 2. (a) Collision-energy-resolved He*(2^3S) PIES of *s*-triazine: solid curve at 86−108 meV, average 100 meV; dotted curve at 136−166 meV, average 150 meV; dashed curve at 220−284 meV, average 250meV. (b) Collision energy dependence of partial ionization cross sections for *s*-triazine with He*(2^3S). Thick lines show experimental data between 90 and 300 meV collision energy, and thin lines indicate theoretical data by trajectory calculations.

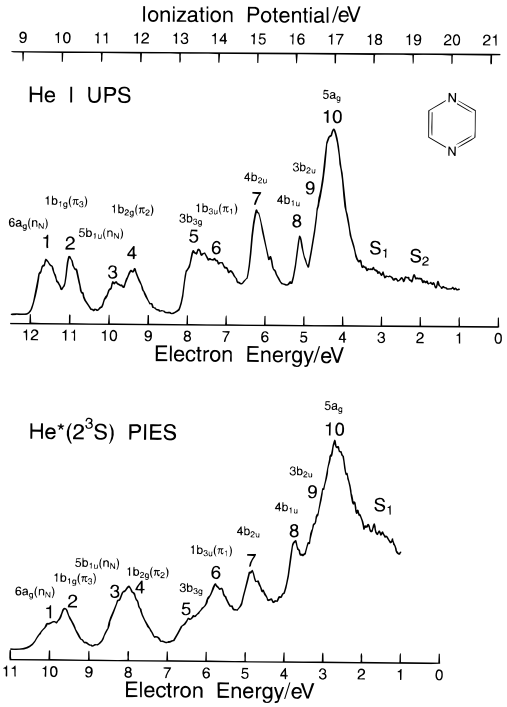

Figure 3. He I UPS and He*(2^3S) PIES of pyrazine.

(2^3S) and Li(2^2S) with various targets.[2,40,41] Because of these findings and difficulties associated with calculations for excited states embedded in ionization continuum, Li atom was used in this study in place of the He(2^3S) atom. The 6-311++G** basis function was used, and the electron correlation energy correction was taken into account by using second-order Mϕller−Plesset perturbation theory (MP2) or DFT with Becke's three-parameter exchange with Lee, Young, Parr correlation function (B3LYP)[42] in order to avoid spin contamination problem. Calculated results were compared for some access directions. All quantum chemical calculations were carried out with the GAUSSIAN 94 program.[43]

Trajectory calculations for ionization of *s*-triazine were performed on three-dimensional potential energy surface obtained by the DFT at more than 300 points utilizing D_{3h} symmetry of the molecule. Ionization width was calculated on the following simplification; Neglecting the angular distribution of the ejected electrons and taking into account that helium 2s orbitals and the continuum orbitals are too diffuse compared to the helium 1s and ionized orbitals, the positional dependence of the ionization width Γ is mainly governed by the more compact 1s and ionized orbitals. The ionization width for each ionic states $\Gamma^{(i)}$, therefore, are represented by

$$\Gamma^{(i)} = K\,|\langle \Phi_i \mid \Psi_{1s} \rangle|^2 \tag{2}$$

where K is a constant, and Φ_i and Ψ_{1s} are the ionized MO and helium 1s orbital, respectively. The impact parameter b was set randomly from 0 to 8 Å for 10 000 trajectories at each collision energy. The molecule is treated as a rigid rotator. The orientation of M was randomly generated, and the initial rotational energy of the molecule was determined with Boltzmann distribution at 300 K. The partial ionization cross section $\sigma^{(i)}$ was obtained from ionization probability $P^{(i)}$ with a weight of $2\pi b\mathrm{d}b$

$$\sigma^{(i)} = 2\pi \int bP^{(i)}\mathrm{d}b \tag{3}$$

Details of the trajectory calculations were reported in previous papers.[26,29] Several K values were attempted for better agreement

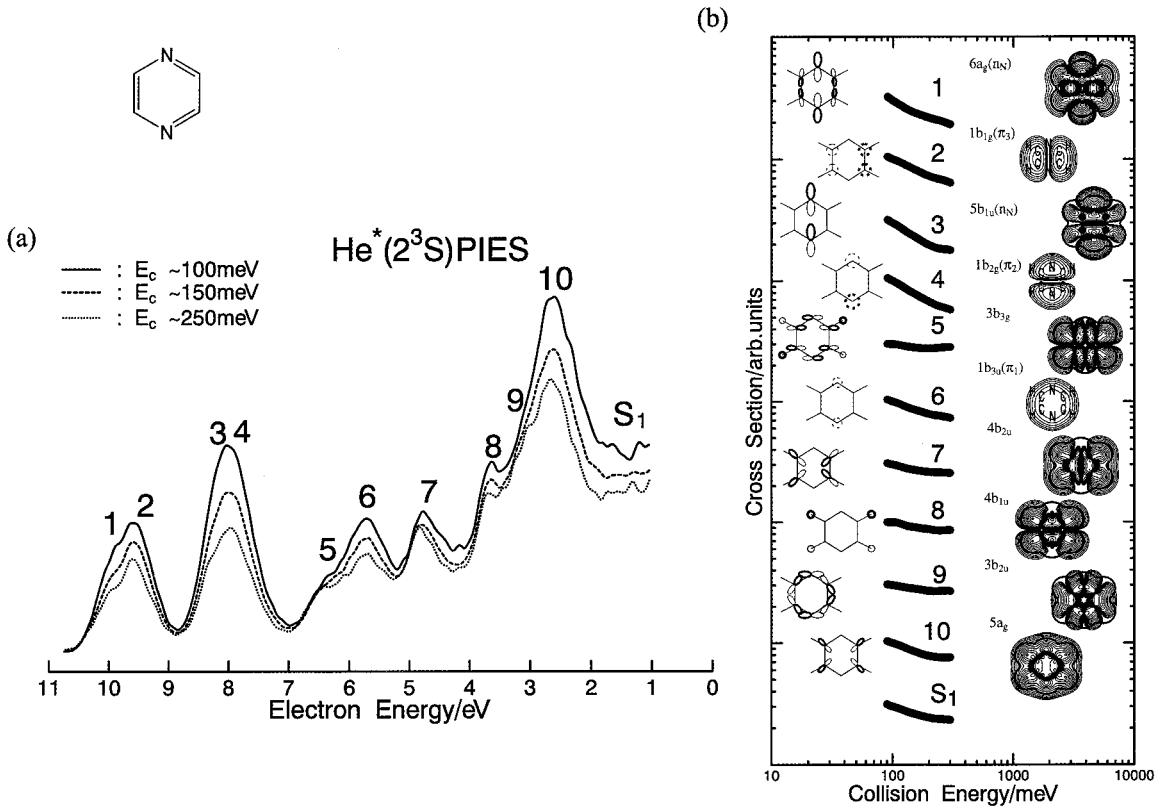

Figure 4. (a) Collision-energy-resolved He*(2^3S) PIES of pyrazine: solid curve at 92−111 meV, average 100 meV; dotted curve at 134−170 meV, average 150 meV; dashed curve at 216−294 meV, average 250meV. (b) Collision energy dependence of partial ionization cross sections for pyrazine with He*(2^3S).

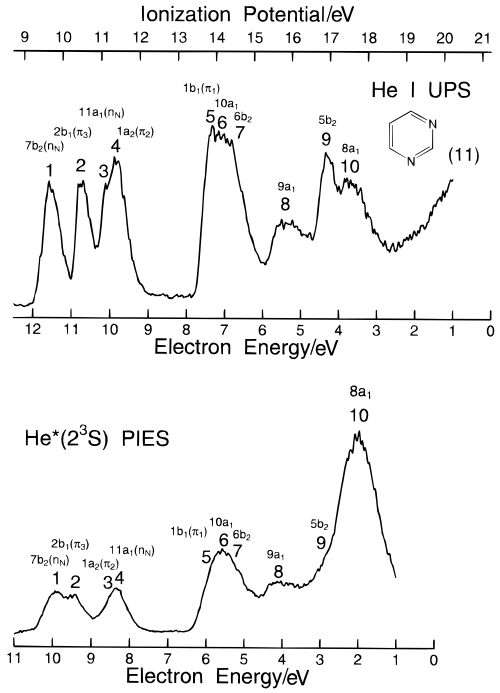

Figure 5. He I UPS and He*(2^3S) PIES of pyrimidine.

of the slope of CEDPICS, because the determination of the unknown *K* value requires the use of at least one experimentally determined physical parameter.

IV. Results

Figures1−10 show He I UPS and He*(2^3S) PIES of target molecules (odd figure numbers) and collision-energy-resolved Penning ionization electron spectrum (CERPIES) and CEDPICS obtained from the two-dimensional data (even figure numbers) of *s*-triazine, pyrazine, pyrimidine, pyridazine, and pyridine. The electron energy scales for PIES are shifted relative to those for the UPS by the difference in the excitation energies, 21.22 − 19.82 = 1.40 eV. The CERPIES are shown for low collision energy (ca. 90−110 meV), middle collision energy (ca. 135−165 meV), and high collision energy (ca. 220−290 meV). The CEDPICS were obtained from the two-dimensional PIES $\sigma(E_e, E_c)$ within an appropriate range of E_e (typically the fwhm of the respective band) to avoid the effect of neighboring bands and shown by the log σ vs log E_c plots in a collision energy range 90−300 meV. Electron density maps are also shown in the figures in order to grasp effective access directions of He*. The calculated electron density maps for σ orbitals are shown on the molecular plane, and those for π orbitals are shown on a plane at a height of 1.70 Å (van der Waals radii of C atom) from the molecular plane. Theoretically obtained CEDPICS for *s*-triazine by trajectory calculation at several collision energies (50, 100, 200, 300, 500, and 700 meV) were shown in Figure 6 in solid line.

Tables1−3 list the vertical ionization potentials (IP determined from the He I UPS) and the assignment of the observed bands for *s*-triazine, diazines (pyrazine, pyrimidine, and pyridazine), and pyridine, respectively. Valence IP values by earlier calculations by post Hartree−Fock methods are also shown. GF is the many body Green's function method,[44] TDA the two-particle-hole Tamm−Dancoff approximation calculations,[44] P3 the partial third-order electron propagator method,[45] and CI the configuration interaction calculations.[46] SAC−CI is based on the symmetry-adapted cluster (SAC)-CI theory.[47] The peak energy shifts (ΔE) in PIES measured with respect to the "nominal" energy E_0 (E_0 = the difference between the metastable excitation energy and the target ionization potential) are also shown in the tables. Values of the slope parameter *m* for the log σ vs log E_c plots estimated in a collision energy range

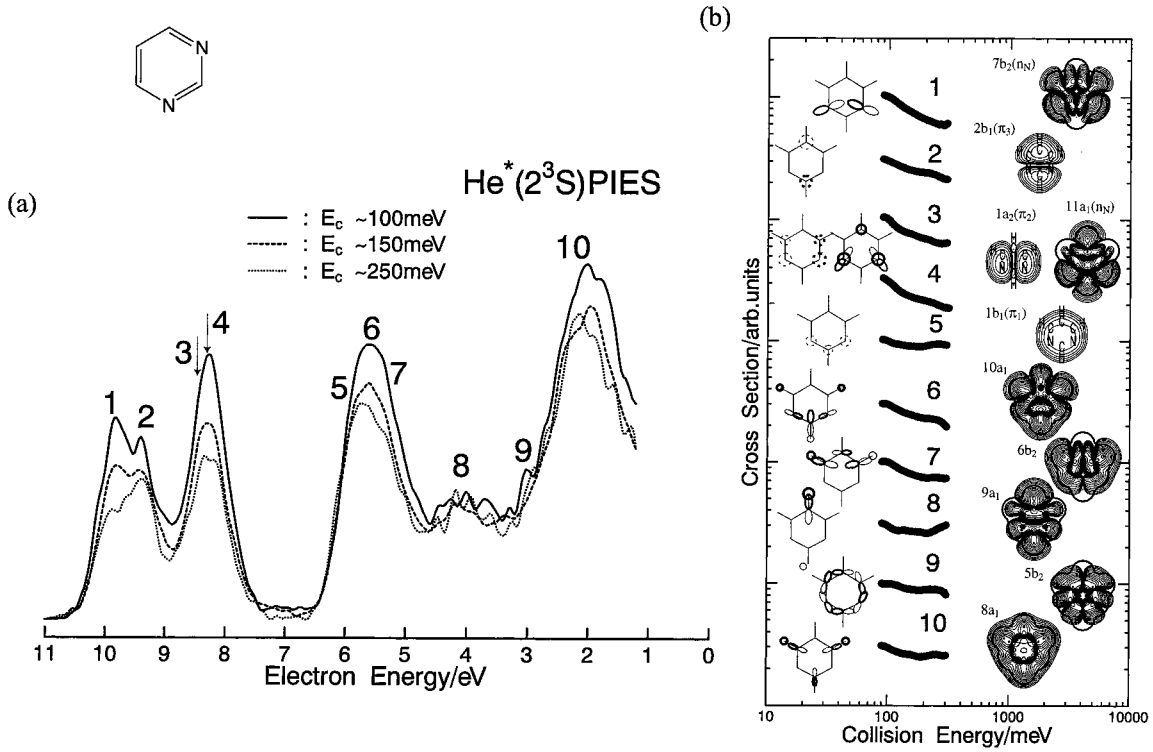

Figure 6. (a) Collision-energy-resolved He*(2^3S) PIES of pyrimidine: solid curve at 94−108 meV, average 100 meV; dotted curve at 137−164 meV, average 150 meV; dashed curve at 222−282 meV, average 250meV. (b) Collision energy dependence of the partial ionization cross sections for pyrimidine with He*(2^3S).

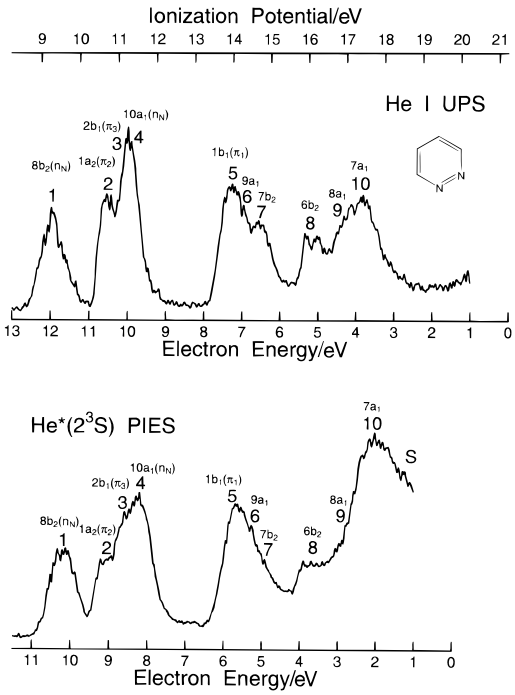

Figure 7. He I UPS and He*(2^3S) PIES of pyridazine.

90−300 meV (100−300 meV for trajectory calculation) by a linear least-squares method are also listed.

Potential energy curves $V(R)$ for in-plane or out-of-plane access were shown in Figures11−12 by the model potential calculations for M−Li system. The distance R between Li and the molecule is measured from the center of the ring.

V. Discussion

Photoelectron spectra of azines have been extensively investigated,[44−59] but there are discrepancies concerning assignments of some bands. On the other hand, electronic structures of these azines also have been investigated theoretically.[44−47,60−69] For the PIES measurement, Penning ionization of pyridine was observed with the Ne*($^3P_2$) atom, and assignment of π_1 band which shows highest IP among π bands was confirmed previously.[70]

A. *s*-Triazine. Ionization from degenerate '"lone-pair" 6e′ (n_N) and 1e" (π) orbitals is observed for band 1 and band 2, respectively. In previous studies of UPS,[53,54] a Jahn−Teller split was observed for band 2, and nitrogen breathing vibrational structure (ν = 1190 cm^{-1}) was reported for band 3 which originates from lone-pair 5a$_1$′ (n_N) orbital. In this study, strong negative collision energy dependence was observed for the two n_N bands (band 1 and 3), while collision energy dependence for band 2 was not stronger than the n_N bands (Figure 2). Clearly different trends were obtained in the calculated CEDPICS for n_N bands (negative dependence) and π band (positive dependence).

As discussed in previous papers,[2,5,10] positive or negative slope of CEDPICS reflects the type of interaction. In the case of attractive interaction, a slower He* atom can approach reactive region more effectively through deflection of its trajectory. For atomic target, it is known that ionization cross section ($\sigma(E_c)$) can be represented as a function of collision energy ($\sigma(E_c) \propto E_c^{-2/s}$) if the long-range attractive part of the interaction potential $V(R)$ plays a dominant role and shown with a potential parameter s ($V(R) \propto R^{-s}$). In the case of repulsive interaction, higher He* can approach reactive inner region of the molecule, which results in positive collision energy dependence of $\sigma(E_c)$.

Actually, negative and positive slopes were obtained by the trajectory calculation reflecting the strong attractive interaction around the nitrogen atoms and repulsive interaction for out-of-plane direction, respectively. Negative peak shifts for band 1 ($\Delta E = -260 \pm 50$ meV) and band 3 ($\Delta E = -210 \pm 50$ meV)

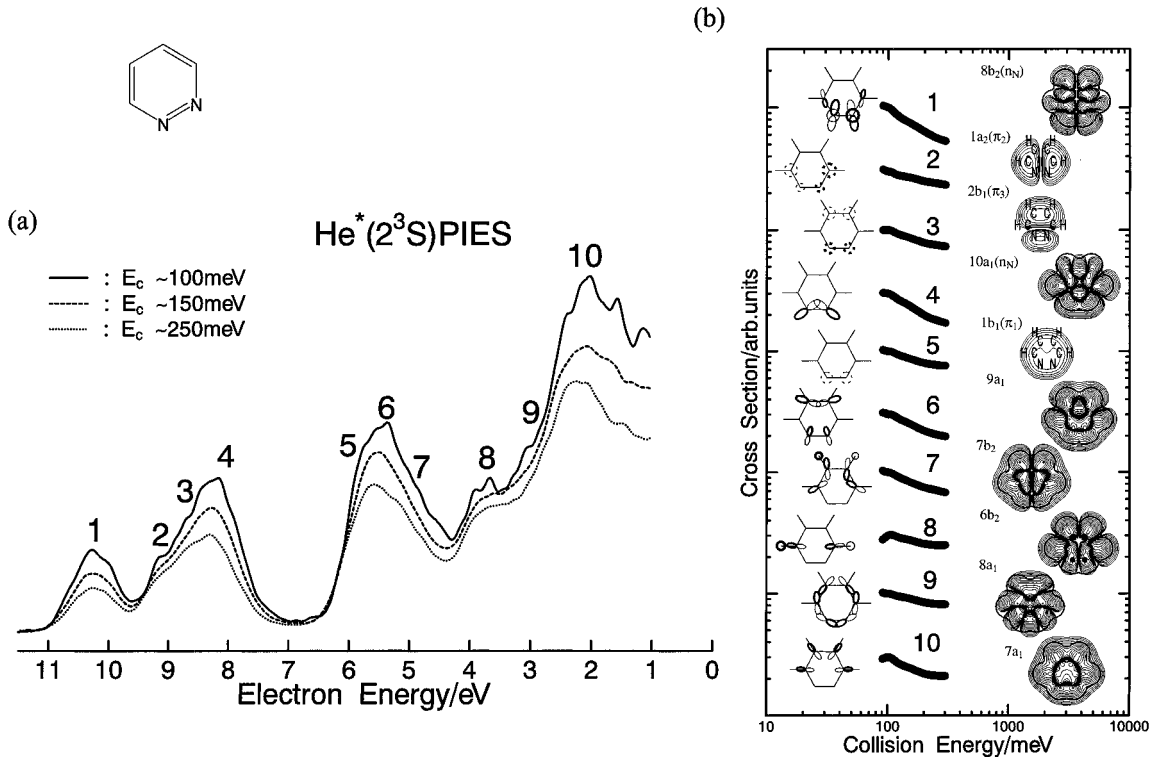

Figure 8. (a) Collision-energy-resolved He*(2^3S) PIES of pyridazine: solid curve at 91−111 meV, average 100 meV; dotted curve at 134−170 meV, average 150 meV; dashed curve at 216−295 meV, average 250meV. (b) Collision energy dependence of partial ionization cross sections for pyridazine with He*(2^3S).

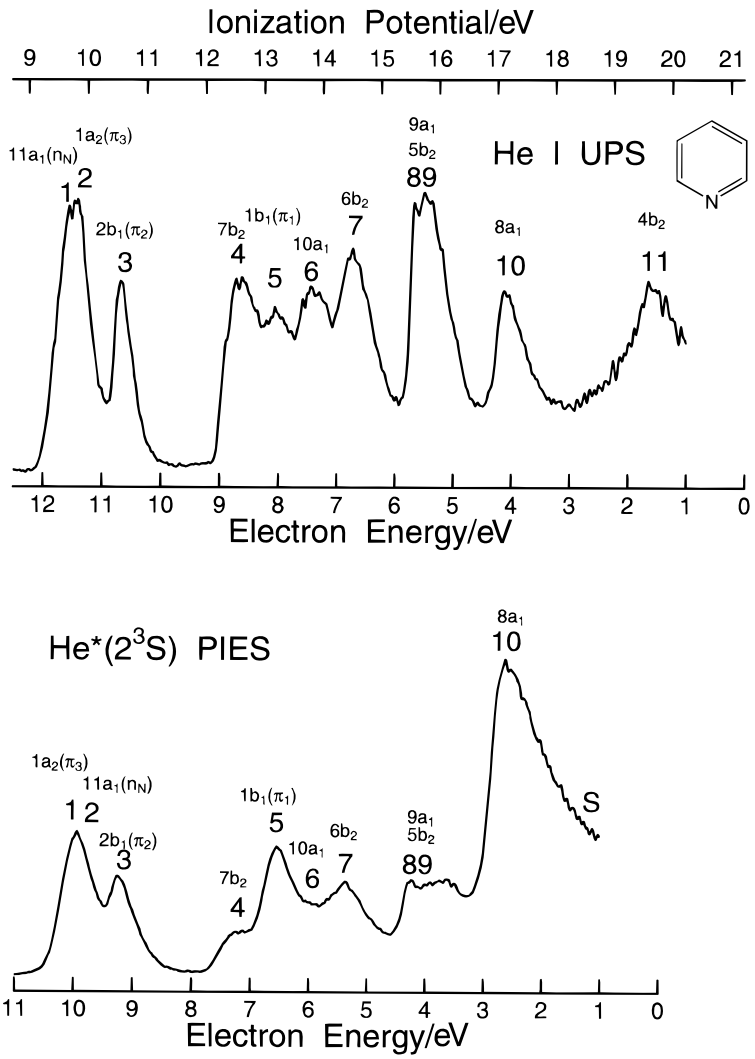

Figure 9. He I UPS and He*(2^3S) PIES of pyridine.

indicate the existence of an attractive well of this order, and the estimated values are on the order of the calculated well depth (Figure 11a). On the other hand, peak shift for band 2 was relatively small ($\Delta E = -100 \pm 75$ meV), which is consistent with the small slope of observed and calculated CEDPICS.

It should be noted that interaction potential energy curves by DFT calculation were quantitatively similar to those by MP2 calculation for in-plane direction access to the N atom and out-of-plane direction access to the ring, while interaction potential calculated for out-of-plane direction of other azines in this study shows a different trend between DFT and MP2 calculations. In addition, since trends of anisotropic interactions were clearly different (attractive interaction around the nitrogen atoms and repulsive interaction around CH bonds and out-of-plane direction) and overlapping of bands 1−3 of *s*-triazine were not observed, significant difference was obtained both for experimental and theoretical CEDPICS.

Discrepancy of the band assignments can be ascribed to overlapping band 4 (IP = 14.7 eV) and band 5 (IP = 14.9 eV, or IP = 15.6 eV in ref 52b). The ordering in IPs of $5e'^{-1}$ and $1a_2''^{-1}$ was uncertain, even by the post Hartree−Fock calculations (Table 1). Anisotropic interaction with a He*(2^3S) atom is useful in the assignment of overlapping bands 4 and 5. A distinct difference was obtained for ionization from $1a_2''$ (π) MO (positive dependence, $m = 0.05$) and $5e'$ MO (negative dependence, $m = -0.15$) in the calculated CEDPICS, reflecting repulsive interaction for out-of-plane direction (ionization from π MO) and attractive interaction for in-plane direction (ionization form $5e'$ MO). Observed results of CEDPICS show small (band 4) and relatively large (band 5) negative dependence, which is in good agreement with the assignment of band 4 to $1a_2''$ (π) and band 5 to $5e'$ MOs (Figure 2). In addition, since a larger negative peak energy shift of band 5 rather than that of band 4 is expected because of the attractive interaction for in-plane direction, the order of ionic states for band 4 and 5 in UPS is thought to be unchanged in PIES.

Large intensity of band 7 can be ascribed to in-phase $4a_1'$ orbital outside the molecular surface in contrast to small intensity of band 6 that ordinates from scarcely extending $1a_2'$ orbital. Similar large bands were also observed for ionization from in-plane orbitals of five-membered heterocyclic compounds,[21c] furan and thiophene. Calculated CEDPICS for ionization from $1a_2'$ and $4a_1'$ MOs shows strong negative dependence reflecting attractive interaction for the in-plane direction around the molecule, while the observed CEDPICS showed weaker dependence rather than n_N bands. This discrepancy may be ascribed to background signals observed in low electron energies or satellite lines where one-particle picture of ionization breaks down as indicated in TDA calcualtion.[44]

B. Diazines. For n_N bands, large differences between excitation energies for cationic states and Koopmans' IPs of diazines show considerable relaxation in ionization relative to π ioniza-

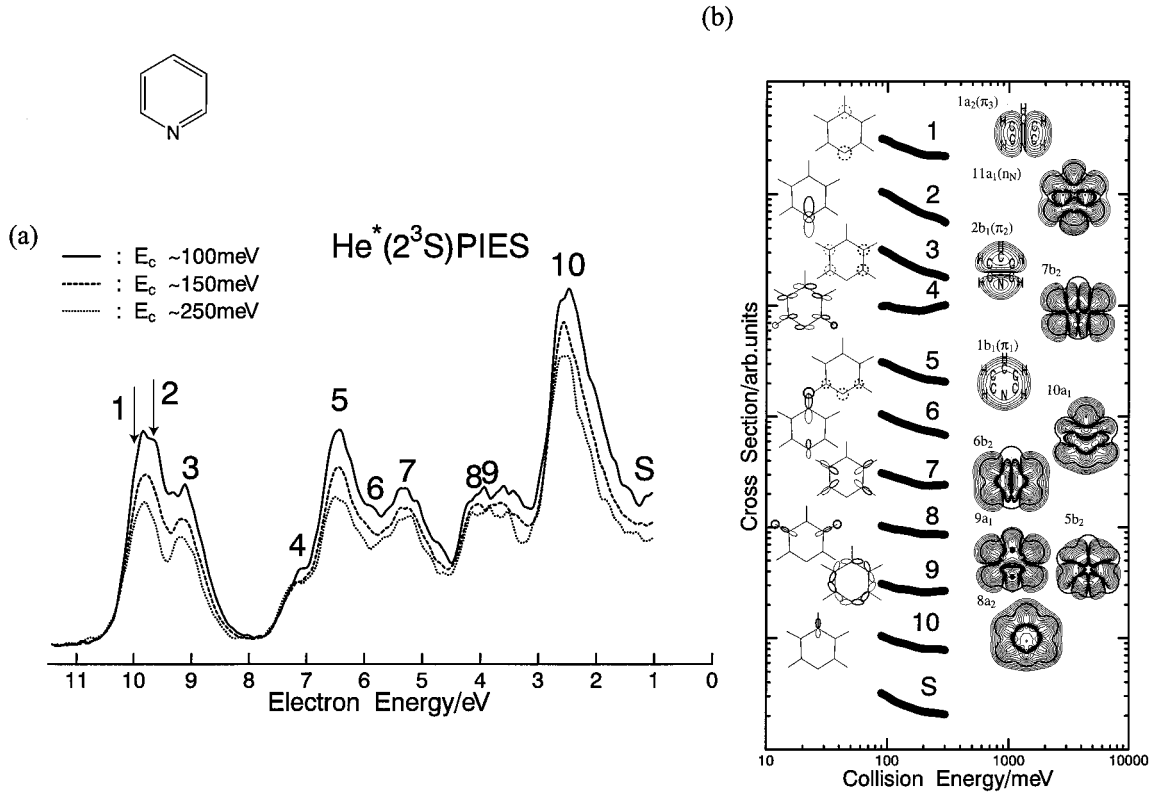

Figure 10. (a) Collision-energy-resolved He*(2^3S) PIES of pyridine: solid curve at 93−107 meV, average 100 meV; dotted curve at 138−163 meV, average 150 meV; dashed curve at 224−281 meV, average 250meV. (b) Collision energy dependence of partial ionization cross sections for pyridine with He*(2^3S).

TABLE 1: Band Assignments, Ionization Potential (IP), Peak Energy Shift (ΔE), Obtained Slope Parameter (m) and Calculated Ionization Potential for s-Triazine (See Text)

band	obs IP/eV	obs ΔE/meV	obs m	calc m	orbital character	Koopman's IP/eV	GF[a] IP/eV	TDA[a] IP/eV	P3[b] IP/eV	CI[c] IP/eV
1	10.40	-260 ± 50	-0.37 ± 0.03	−0.28	6e′(n_N)	10.90	10.31	10.72	10.550	9.877
2	11.79	-100 ± 5	-0.15 ± 0.03	−0.06	1e″(π)	11.79	12.01	11.98	12.104	11.731
3	13.37	-210 ± 50	-0.31 ± 0.06	−0.18	5a$_1$′(n_N)	14.78	13.25	14.28	13.521	12.589
4	14.64	-50 ± 100	-0.01 ± 0.06	−0.05	1a$_2$′(π)	16.64	15.68	15.22	15.593	14.958
5	14.99	-200 ± 100	-0.13 ± 0.03	−0.15	5e′	17.85	15.37	15.66	15.429	15.294
6	17.6		-0.02 ± 0.05	−0.49	1a$_2$′	20.21		18.50, 18.86[d]	18.714	16.639
7	18.31	-50 ± 100	-0.09 ± 0.03	−0.30	4a$_1$′	21.02		19.72[d], 19.84	18.919	

[a] Reference 44. [b] Reference 45. Results with correlation consistent triple-ζ basis set are listed. [c] Reference 46e. Shake-up states were calculated in 13 < IP < 18 eV region. [d] Main peak.

tion. Band 3 (n_N) and band 4 (π) of diazines lie close together in UPS and PIES (Figures 3, 5, and 7). Assignments of the first four bands mostly agree within the post Hartree−Fock calculations[44−46] to a sequence of $n_N < \pi_3 < n_N < \pi_2$ in the IP order for pyrazine and pyrimidine and to $n_N < \pi_3 < \pi_2 < n_N$ for pyridazine. Moreover, first four bands of pyrazine and pyrimidine were also assigned to $n_N < \pi_3 < n_N < \pi_2$ by observing angular distribution parameter in photoelectron spectroscopy.[58,59] On the other hand, the orderings of valence IPs for band 5 and band 6 of diazines seem to be uncertain even by the post Hartree−Fock calculations (Table 2). In addition, relatively low pole strength for ionization from π_1 orbital of these samples was calculated.[44,45] In higher ionization potential energy range than 16 eV, many satellite lines or shake-up states were suggested by the TDA,[44] P3,[45] and CI[46b−d] calculations.

As observed CEDPICS of pyrimidine (Figure 6) and pyridazine (Figure 8) for band 1 (n_N, the slope parameter is between ca. −0.5 to −0.6) and band 2 (π_3, the slope parameter is between ca. −0.2 to −0.3), clear difference was observed in ionization for in-plane and out-of-plane direction. Interaction potential calculations (Figure 12) show attractive curves for in-plane direction with well depth more than 450 meV. On the other hand, repulsive interaction was calculated by MP2 method for out-of-plane direction and difficulty in SCF convergence occurred at short distance. Weak interaction was indicated by peak energy shift and CEDPICS for π bands of pyrimidine and pyridazine. It should be noted that the negative peak energy shift values for π bands of pyridazine (−80 meV in average) are larger than those of pyrimidine (positive or near zero), which qualitatively agrees with the potential energy curve for out-of-plane direction by DFT method with well depth for pyridazine (350 meV) and pyrimidine (160 meV).

For pyrazine, however, significant difference was not observed for strong negative collision energy dependence of band 1 (n_N) and band 2 (π_3) (Figure 4), which also agrees with the attractive interaction calculated for in-plane and out-of-plane directions by MP2 and DFT calculations (Figure 12a). In addition, strong negative collision energy dependence for band 6 (π_1, $m = -0.31 \pm 0.05$) and large negative peak energy shift

TABLE 2: Band Assignments, Ionization Potential (IP), Peak Energy Shift (Δ*E*), Obtained Slope Parameter (*m*) and Calculated Ionization Potential for Diazines (See Text)

	obs			orbital	Koopman's	GF[a]	TDA[a]	P3[b]	CI[c]
band	IP/eV	Δ*E*/meV	*m*	character	IP/eV	IP/eV	IP/eV	IP/eV	IP/eV
pyrazine									
1	9.61	−270 ± 40	−0.41 ± 0.06	$6a_g(n_{N+})$	10.88	9.21	8.96	9.788	9.01
2	10.20	−200 ± 50	−0.43 ± 0.03	$1b_{1g}(\pi_3)$	10.08	10.18	9.87	10.290	10.08
3	11.38	−170± 50	−0.54 ± 0.07	$5b_{1u}(n_{N-})$	13.44	11.04	10.59	11.573	10.84
4	11.80	−220 ± 80	−0.53 ± 0.03	$1b_{2g}(\pi_2)$	11.90	11.62	11.23	12.013	11.65
5	13.37	30 ± 75	−0.07 ± 0.05	$3b_{3g}$	15.11	13.69	13.54	13.984	14.00
6	13.93	−110 ± 20	−0.31 ± 0.05	$1b_{3u}(\pi_1)$	15.81	14.40	13.66	14.441	13.87
7	14.98	0 ± 60	−0.16± 0.04	$4b_{2u}$	16.87	15.39	15.29	15.229	14.11
8	16.10	−10 ± 40	−0.16 ± 0.04	$4b_{1u}$	18.50		16.55[d], 16.67	16.791	16.32
9	16.58	−50 ± 100	−0.13 ± 0.03	$3b_{2u}$	19.35		16.16, 17.29[d]	17.467	17.03
10	16.97	−130 ± 20	−0.30 ± 0.06	$5a_g$	19.93		17.12, 17.51[d]	17.747	16.21
S_1	(18.0)		−0.26 ± 0.05						
S_2	(19.1)								
pyrimidine									
1	9.69	−250 ± 75	−0.53 ± 0.07	$7b_2(n_{N-})$	11.00	9.50	9.86	9.863	9.351
2	10.50	100 ± 70	−0.29 ± 0.04	$2b_1(\pi_3)$	10.46	10.54	10.43	10.647	10.412
3	11.22	(−250)	(−0.43 ± 0.10)	$11a_1(n_{N+})$	12.61	10.87	11.15	11.334	10.713
4	11.40	(100)	(−0.42 ± 0.10)	$1a_2(\pi_2)$	11.40	11.23	11.16	11.576	11.292
5	13.9	10 ± 100	−0.06 ± 0.08	$1b_1(\pi_1)$	15.68	14.46	13.95[d], 20.79	14.558	14.015
6	14.1	−120 ± 100	−0.32 ± 0.05	$10a_1$	16.20	14.25	14.46	14.557	14.916
7	14.4	−100 ± 100	−0.31 ± 0.10	$6b_2$	16.42	14.40	14.73	14.726	15.007
8	15.8	10 ± 150	−0.06 ± 0.12	$9a_1$	17.84	16.02	16.31	16.162	16.303
9	16.88	0 ± 200	−0.13 ± 0.04	$5b_2$	19.12		17.23[d], 17.52	17.450	18.049
10	17.4	−360 ± 150	−0.15 ± 0.10	$8a_1$	20.31		18.22	18.228	17.663
11	(20.5)			$7a_1$	24.31		21.92[d], 22.27		
pyridazine									
1	9.27	−350 ± 50	−0.59 ± 0.04	$8b_2(n_{N-})$	10.83	8.79	9.08	9.284	8.523
2	10.61	−100 ± 75	−0.22 ± 0.02	$1a_2(\pi_3)$	10.65	10.62	10.44	10.853	10.697
3	11.2	−50± 75	−0.30 ± 0.03	$2b_1(\pi_2)$	11.11	11.11	11.00	11.287	10.872
4	11.3	−340 ± 100	−0.57 ± 0.03	$10a_1(n_{N+})$	12.91	11.20	11.44	11.656	10.679
5	13.97	−90 ± 75	−0.27 ± 0.03	$1b_1(\pi_1)$	15.83	14.42	13.83[d], 20.80	14.554	13.776
6	14.27	−200 ± 50	−0.43 ± 0.04	$9a_1$	16.10	14.13	14.45	14.519	13.367
7	14.66	−200 ± 75	−0.37 ± 0.04	$7b_2$	16.51	14.95	15.25	14.880	14.239
8	15.90	−30 ± 75	−0.20 ± 0.03	$6b_2$	18.33	16.47	16.70	16.517	16.502
9	16.8		−0.21 ± 0.03	$8a_1$	19.15	18.16	17.26	17.390	16.888
10	17.43	−370 ± 150	−0.35 ± 0.06	$7a_1$	20.15		18.57	17.959	17.300

[a] Reference 44. [b] Reference 45. Results with correlation consistent triple-ζ basis set are listed. [c] Reference 46b−d. Shake-up states were calculated in the IP > 12 eV region. [d] Main peak.

TABLE 3: Band Assignments, Ionization Potential (IP), Peak Energy Shift (Δ*E*), Obtained Slope Parameter (*m*), and Calculated Ionization Potential for Pyridine (See Text)

	obs			orbital	Koopman's	GF[a]	TDA[a]	P3[b]	ADC(3)[c]	CI[d]	SAD-CI[e]
band	IP/eV	Δ*E*/meV	*m*	character	IP/eV	IP/eV	IP/eV	IP/eV	IP/eV	IP/eV	IP/eV
1	9.67	(−500)	−0.54 ± 0.06	$11a_1(n_N)$	11.08	9.59	9.64	9.849	9.78	8.843	8.96
2	9.85	(−40)	−0.34 ± 0.07	$1a_2(\pi_3)$	9.55	9.57	9.45	9.827	9.44	9.526	9.38
3	10.52	−50 ± 50	−0.49 ± 0.07	$2b_1(\pi_2)$	10.37	10.24	10.15	10.596	10.15	10.127	9.95
4	12.60	−50 ± 75	−0.03 ± 0.10	$7b_2$	13.95	12.87	12.97	13.039	12.73	12.908	12.12
5	13.19	−90 ± 25	−0.38 ± 0.06	$1b_1(\pi_1)$	14.74	13.43	12.90	13.536	13.18[f]	13.044	13.20[f], 20.77
6	13.79	−40 ± 75	−0.36 ± 0.06	$10a_1$	15.72	14.18	14.26	14.114	13.92[f]	13.696	13.46
7	14.51	70 ± 50	−0.26 ± 0.07	$6b_2$	16.36	15.11	15.14	14.843	14.65[f]	14.636	14.34
8,9	15.6		(−0.16± 0.04)	$9a_1$[g]	17.71	16.32	16.26	16.111	16.02[f]	16.048	15.75
	15.8		(−0.13± 0.07)	$5b_2$[g]	17.98		16.05, 16.31[f]	16.284	16.18[f]	15.497	15.38
10	17.10	−120 ± 50	−0.25 ± 0.06	$8a_1$	19.74		17.94[f], 18.40	17.720	17.60[f]		17.25[f], 17.37
S	(18.5)		−0.37 ± 0.06								
11	19.6			$4b_2$	23.29		21.16, 21.32[f]		20.44[f]		20.50

[a] Reference 44. [b] Reference 45. Results with correlation consistent triple-ζ basis set are listed. [c] Reference 69. Satellite lines were calculated in IP > 14.0 eV region. [d] Reference 46a. Shake-up states were calculated in IP > 13.9 eV region. [e] Reference 47. [f] Main peak. [g] Assignments are uncertain.

were observed for π bands. The attractive interaction potential for out-of-plane direction of pyrazine can be ascribed to short-range interorbital interaction between the s component of Li and HOMO that is in-phase in the ring, which was confirmed by checking the molecular orbital component of the interacting system. In contrast to pyrazine, HOMOs of other azines in this study were not in-phase in the ring.

For band 3 and band 4 of pyrimidine, taking large negative peak energy shift of n_N band (band 1) and positive peak energy shift of π band (band 2) into account, peak position of n_N band (ca. 8.35 eV(= 19.82 − IP + Δ*E*)) in PIES can be lower electron energy than π band (ca. 8.52 eV). Both peak positions are indicated by arrows in CERPIES (Figure 6). The slope of CEDPICS for lower electron energy region of strongly overlapping bands 3,4 in PIES ($m = -0.43 \pm 0.10$) was not different from that of higher electron energy region of bands 3,4 ($m = -0.42 \pm 0.10$). Therefore, bands 3 and 4 in PIES are difficult to be assigned to the particular MO. On the other hand, for

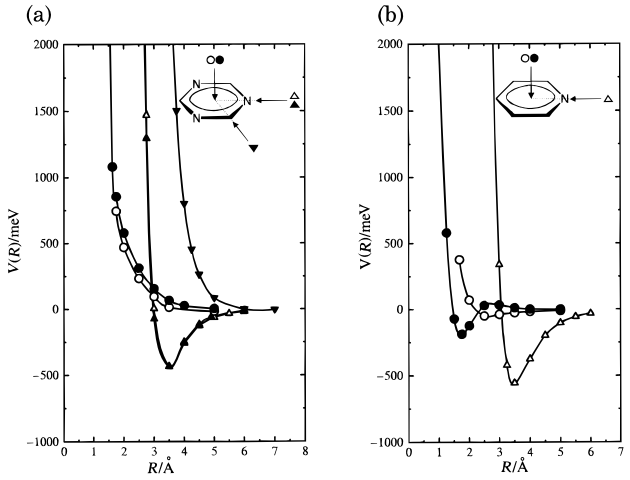

Figure 11. Interaction potential energy curves for (a) *s*-triazine−Li and (b) pyridine−Li: in-plane access to the N atom by MP2 calculation (△) and DFT (B3LYP) calculation (▲); in-plane access to the H atom by DFT (B3LYP) calculation (▼); out-of-plane access to the center of the ring by MP2 calculation (○) and DFT (B3LYP) calculation (●).

pyridazine, large negative peak energy shift of band 4 (n_N band, $\Delta E = -340 \pm 100$ meV) makes it easy to observe significant difference in CEDPICS for band 3 (π_2, $m = -0.30 \pm 0.03$) and band 4 ($m = -0.57 \pm 0.03$) (Figure 8).

For overlapping bands 5−7 of diazines, assignment for π_1 orbital is useful for checking the results of the ionization potential energy calculations. Referring relatively weak negative CEDPICS and small peak energy shift, band 5 of pyrimidine (Figure 6) and pyridazine (Figure 8) can be assigned to the π_1 orbital. Stronger negative slope of CEDPICS for band 6 and band 7 of pyrimidine or pyridazine rather than π band can be ascribed to ionization for in-plane direction, which is similar to the case of *s*-triazine. On the other hand, strong attractive interaction for out-of-plane direction of pyrazine results in negative slope for π_1 band as mentioned above. Weak slope of CEDPICS for band 5 of pyrazine ($m = -0.07 \pm 0.05$) can be ascribed to repulsive interaction around σ_{CH} region where the $3b_{3g}$ orbital extends (Figure 4). Relatively weak negative slope of CEDPICS for band 7 and 8 (σ_{CH} band) of pyrazine can be ascribed to repulsive interaction around the σ_{CH} bond and effects of background signals lower than 5 eV in electron energy.

Band 8 of pyrimidine (Figure 5) and pyridazine (Figure 7) in PIES shows similar shape, and both can be ascribed to σ_{CH} orbital. Vibrational structure of band 8 in PIES was observed in CERPIES of pyrimidine, while vibrational progressions at each collision energy are thought to be composed in PIES. The small slope of CEDPICS for the band 8 ($m = -0.06 \pm 0.12$) of pyrimidine and increasing trend of the cross section in higher collision energies are consistent with repulsive interaction around the corresponding σ_{CH} bonds. On the other hand, for band 8 of pyridazine, the slope of CEDPICS (Figure 8) shows relatively stronger negative slope ($m = -0.20 \pm 0.03$). This may be ascribed to the effect of the strong attractive interaction around neighboring two N atoms.

A common character of enhanced band intensity for band 10 with respect to band 9 was observed also for diazines, which is thought to reflect ionization from extending a_g or a_1 MOs. It should be noted that split lines are calculated in bands 8−10 region of pyrazine according to TDA calculation.[44]

At lower electron energy region than 4 eV in He I UPS of pyrazine (Figure 7), satellite bands labeled $S_1$and S_2 were observed, and CEDPICS of the S_1 band shows negative dependence ($m = -0.26 \pm 0.05$). In He I UPS of pyrimidine (Figure 5), shoulder of band was observed at lower electron energy region than 3 eV, which can be ascribed to band at 20.5 eV in IP observed by He II UPS.[52d]

C. Pyridine. Assignment of first three bands in UPS has been confirmed to be IP order $n_N < \pi_3 < \pi_2$ by angle-resolved measurement of photoelectrons.[56,58] In addition, the ionic ground state is determined to be due to ionization from the nonbonding orbital by multiphoton ionization spectroscopy.[54] However, theoretical calculations[44,45,46a,47,69] show inconsistent results concerning the first two ionization states as shown in Table 3 (ADC(3) is Green function calculation including third-order electron correlation effect[69]). In He*(2^3S) PIES, negative collision energy dependence ($m = -0.49 \pm 0.07$) and small negative peak shift ($\Delta E = -50 \pm 50$ meV) was observed for band 3 (π_2) (Figures 9 and 10). On the other hand, a strong attractive interaction with the well depth of more than 500 meV was calculated for the straight access to the nitrogen atom (Figure 11b). If we assume the peak energy shift for ionization from n_N ($\Delta E = -500$ meV) and π_1 ($\Delta E = -50$ meV), bands 1 and 2 can be assigned to π_3 orbital (9.92 eV (= 19.82 − IP + ΔE) in electron energy) and n_N orbital (9.65 eV), respectively. Both peak positions are indicated by arrows in CERPIES (Figure 10). The slope of CEDPICS for higher electron energy region ($m = -0.34 \pm 0.07$) is similar to that of band 5 ($m = -0.38 \pm$

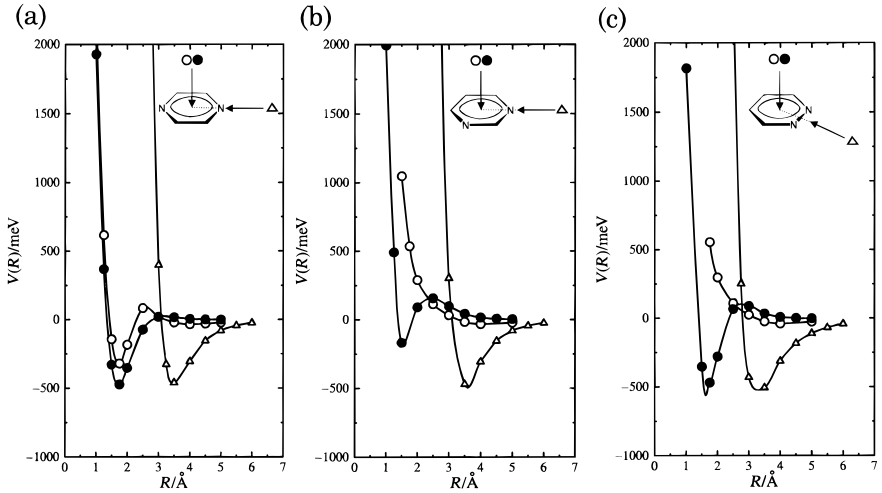

Figure 12. Interaction potential energy curves for (a) pyrazine-Li, (b) pyrimidine-Li, and (c) pyridazine-Li: in-plane access to the N atom (or the center of N atoms for pyridazine) by MP2 calculation (△); out-of-plane access to the center of the ring by MP2 calculation (○) and DFT (B3LYP) calculation (●).

0.06) that was confirmed to ionization from π_1 orbital by the angle-resolved UPS[55] and PIES by metastable Ne* atom.[70] In addition, large negative collision energy dependence of lower electron energy region ($m = -0.54 \pm 0.06$) of bands 1,2 can be ascribed to the strong interaction around the nitrogen atom. Interaction potential energy curve for out-of-plane access is deformed downward by the weak attractive interaction with well depth of ca. 50 meV (MP2) or 180 meV (DFT) that is consistent value with the peak energy shift for π bands comparing with the deep well around the nitrogen atom. It should be noted that in case of benzene−Li, attractive interaction potential well with depth of ca. 200 meV was calculated for out-of-plane direction by MP2 method and negative slope ($m \sim -0.3$) was observed for π bands of benzene.[21a]

Collision energy dependence of band 4 shows small slope ($m = -0.03 \pm 0.10$), which reflects repulsive interaction around σ_{CH} orbital region similarly to σ_{CH} bands of benzene ($m \sim 0.0$).[21a] On the other hand, relatively strong negative collision energy dependence was observed for ionization from another σ_{CH} orbital, band 7 ($m = -0.26 \pm 0.07$). Existence of a shake-up state near band 5 (π_1) was discussed by previous theoretical studies.[45,46a,49,69] Thus we can interpret the reason of this inconsistency concerning the negative slope of band 7 as the shake-up state within the electron energy region for bands 6−7.

The orderings of IPs for ionization from $9a_1$ and $5b_2$ MOs are in disagreement by the post Hartree−Fock calculations (Table 3), and TDA calculation suggested split peaks. Since the $5b_2$ orbital is scarcely extending outside of the molecular surface, the small negative collision energy dependence of bands 8,9 observed in CEDPICS and CERPIES (Figure 10) may be ascribed mainly to ionization from the $9a_1$ orbital. In this study, the assignment of bands 8,9 are still uncertain. The large intensity of band 10 can be ascribed to $8a_1$ MO that is extending in-phase outside the molecular surface. The broadness of band 10 can be ascribed to the split of peaks proposed by some calculations.[44,47,69] The negative slope of CEDPICS ($m = -0.25 \pm 0.06$) is consistent with the attractive interaction for the in-plane direction around the N atom.

On the other hand, satellite band labeled S was observed around 1.5 eV in PIES. The S band shows negative collision energy dependence ($m = -0.37 \pm 0.06$), which can be related to π ionization because of the similarity in slope of CEDPICS with π_1 band ($m = -0.38 \pm 0.06$) and calculated results by SAC−CI[47] and ADC(3).[69] It should be noted that the shake-up state was observed in PIES of benzene with negative slope of CEDPICS in electron energy of 3.7 eV.[19,21a]

VI. Conclusion

Different behavior (positive or negative slope) of collision energy dependence of the partial ionization cross sections (CEDPICS) observed by the collision-energy-resolved Penning ionization electron spectroscopy indicates anisotropic interactions around the molecule with a He* atom. Attractive interaction around the N atoms and repulsive interaction for the out-of-plane directions were found by 2D-PIES of *s*-triazine, which was confirmed by theoretically through interaction potential energy calculations by DFT (B3LYP) and classical trajectory calculations on the anisotropic three-dimensional potential energy surface. Attractive interaction was also found around the N atoms of other azines investigated, while interaction for out-of-plane directions was found to be weakly attractive for pyrimidine, pyridazine, and pyridine rather than benzene or strongly attractive for pyrazine. In other words, attractive interaction decreases as the number of nitrogen atoms in the ring increases from benzene to *s*-triazine, except for pyrazine. For all sample molecules, interaction around the σ_{CH} bond was found to be repulsive.

Obtained information on the anisotropic interaction around the molecule leads to reasonable assignment of photoelectron spectra. Utilizing positive slope of CEDPICS reflecting repulsive interaction for out-of-plane direction and negative slope of CEDPICS reflecting attractive interaction for in-plane direction, we have assigned the overlapping band 4 and band 5 of *s*-triazine to ionization from $1a_2''(\pi)$ MO and 5e′ MO, respectively. Similarly, different slope of CEDPICS was useful in assignment of n_N and π bands for diazines and pyridine. Negative collision energy dependence was observed for shake-up states in lower electron energy region of PIES for pyrazine and pyridine.

Acknowledgment. This work has been supported by a Grant in Aid for Scientific Research from the Japanese Ministry of Education, Science, and Culture.

References and Notes

(1) Penning, F. M. *Naturwissenshaften* **1927**, *15*, 818.
(2) Niehaus, A. *Adv. Chem. Phys.* **1981**, *45*, 399.
(3) Yencha, A. J. *Electron Spectroscopy: Theory, Technique, and Applications*, Brundle, C. R., Baker, A. D., Eds.; Academic: New York, 1984; Vol. 5.
(4) Siska, P. E., *Rev. Mod. Phys.* **1993**, *65*, 337.
(5) Illenberger, E.; Niehaus, A. *Z. Phys. B* **1975**, *20*, 33.
(6) Parr, T. P.; Parr D. M.; Martin, R. M. *J. Chem. Phys.* **1982**, *76*, 316.
(7) Pesnelle, A.; Watel, G.; Manus, C. *J. Chem. Phys.* **1975**, *62*, 3590.
(8) Woodard, M. R.; Sharp, R. C.; Seely, M.; Muschlitz, E. E., Jr. *J. Chem. Phys.* **1978**, *69*, 2978.
(9) Appoloni, L.; Brunetti, B.; Hermanussen, J.; Vecchiocattivi F.; Volpi, G. G. *J. Chem. Phys.* **1987**, *87*, 3804.
(10) Allison, W.; Muschlitz, E. E., Jr. *J. Electron Spectrosc. Relat. Phenom.* **1981**, *23*, 339.
(11) Riola, J. P.; Howard, J. S.; Rundel R. D.; Stebbings, R. F. *J. Phys. B* **1974**, *7*, 376.
(12) Lindinger, W.; Schmeltekopf, A. L.; Fehsenfelt, F. C. *J. Chem. Phys.* **1974**, *61*, 2890.
(13) Hotop, H.; Niehaus, A. *Z. Phys.* **1969**, *228*, 68.
(14) Cermak, V. *J. Chem. Phys.* **1966**, *44*, 3781.
(15) Ohno, K.; Mutoh, H.; Harada, Y. *J. Am. Chem. Soc.* **1983**, *105*, 4555.
(16) Ohno, K.; Takami, T.; Mitsuke, K.; Ishida, T. *J. Chem. Phys.* **1991**, *94*, 2675.
(17) Ohno, K.; Yamakado, H.; Ogawa, T.; Yamata, T. *J. Chem. Phys.* **1996**, *105*, 7536.
(18) (a) Mitsuke, K.; Takami, T.; Ohno, K. *J. Chem. Phys.* **1989**, *91*, 1618. (b) Kishimoto, N.; Furuhashi, M.; Ohno, K. *J. Electron Spectrosc. Relat. Phenom.* **1998**, *88*−*91*, 143.
(19) Takami, T.; Ohno, K. *J. Chem. Phys.* **1992**, *96*, 6523.
(20) (a) Pasinszki, T. Yamakado, H.; Ohno, K. *J. Phys. Chem.* **1993**, *97*, 12718. (b) Pasinszki, T.; Yamakado, H.; Ohno, K. *J. Phys. Chem.* **1995**, *99*, 14678. (c) Yamakado, H.; Yamauchi, M.; Hoshino, S.; Ohno, K. *J. Phys. Chem.* **1995**, *99*, 17093. (d) Ohno, K.; Okamura, K.; Yamakado, H.; Hoshino, S.; Takami, T. *J. Phys. Chem.* **1995**, *99*, 14247. (e) Kishimoto, N.; Yokoi, R.; Yamakado, H.; Ohno, K. *J. Phys. Chem. A* **1997**, *101*, 3284. (f) Pasinszki, T.; Kishimoto, N.; Ohno, K. *J. Phys. Chem. A* **1999**, *103*, 6746. (g) Pasinszki, T.; Kishimoto, N.; Ohno, K. *J. Phys. Chem. A* **1999**, *103*, 9195. (h) Kishimoto, N.; Osada, Y.; Ohno, K. *J. Phys. Chem. A* **2000**, *104*, 1393.
(21) (a) Yamakita, Y.; Yamauchi M.; Ohno, K. *Chem. Phys. Lett.* **2000**, *322*, 189. (b) Yamauchi, M.; Yamakita, Y.; Yamakado, H.; Ohno, K. *J. Electron Spectrosc. Relat. Phnom.* **1998**, *88*−*91*, 155. (c) Kishimoto, N.; Yamakado H.; Ohno, K. *J. Phys. Chem.* **1996**, *100*, 8204.
(22) Tanaka H.; Yamakado, H.; Ohno, K. *J. Electron Spectrosc. Relat. Phenom.* **1998**, *88*−*91*, 149.
(23) (a) Hickman, A. P.; Isaacson, A. D.; Miller, W. H. *J. Chem. Phys.* **1977**, *66*, 1483, 1492. (b) Isaacson, A. D.; Hickman, A. P.; Miller, W. H. *J. Chem. Phys.* **1977**, *67*, 370. (c) Cohen, J. S.; Lane, N. F. *J. Phys. Chem.* **1977**, *66*, 586. (d) Vojtik, J. *Chem. Phys.* **1996**, *209*, 367.
(24) (a) Ishida, T. *Chem. Phys. Lett.* **1993**, *211*, 1. (b) Ishida, T.; Horime, K. *J. Chem. Phys.* **1996**, *105*, 5380.
(25) Dunlavy, D. C.; Siska, P. E.; *J. Phys. Chem.* **1996**, *100*, 21.
(26) Ogawa, T.; Ohno, K. *J. Chem. Phys.* **1999**, *110*, 3773.

(27) (a) Brunetti, B.; Candori, P.; De Andres, J.; Pirani, F.; Rosi, M.; Falcinelli, S.; Vecchiocattivi, F. *J. Phys. Chem. A* **1997**, *101*, 7505. (b) Alberti, M.; Lucas J. M.; Brunetti, B.; Pirani, F.; Stramaccia, M.; Rosi, M.; Vecchiocattivi F. *J. Phys. Chem. A* **2000**, *104*, 1405.

(28) Pasinszki, T.; Kishimoto, N.; Ogawa, T.; Ohno, K. *J. Phys. Chem. A* **1999**, *103*, 7170.

(29) Ogawa, T.; Ohno, K. *J. Phys. Chem. A*, **1999**, *103*, 9925.

(30) Takami, T.; Mitsuke, K.; Ohno, K. *J. Chem. Phys.* **1991**, *95*, 918.

(31) Gardner, J. L.; Samson, J. A. R. *J. Electron Spectrosc. Related. Phenom.* **1976**, *8*, 469.

(32) Kimura, K.; Katsumata, S.; Achiba, Y.; Yamazaki, T.; Iwata, S. *Handbook of He I Photoelectron Spectra of Fundamental Organic Molecules*; Japan Scientific: Tokyo, 1981.

(33) (a)Auerbach, D. J. *Atomic and Molecular Beam Methods*; Scoles, G., Ed.; Oxford University: New York, 1988; p 369. (b) Kishimoto, N.; Aizawa, J.; Yamakado, H.; Ohno, K. *J. Phys. Chem. A* **1997**, *101*, 5038.

(34) Pyckout, W.; Callaerts, I.; van Alsenoy, C.; Geise, H. J.; Almenningen, A.; Seip, R. *J. Mol. Struct.* **1986**, *147*, 321.

(35) Cradock, S.; Liescheski, P. B.; Rankin, D. W. H.; Robertson, H. E. *J. Am. Chem. Soc.* **1988**, *110*, 2758.

(36) Cradock, S.; Purves, C.; Rankin, D. W. H. *J. Mol. Struct.* **1990**, *220*, 193.

(37) Bak, B.; Hansen, L.; Rastrup-Andersen, J. *J. Chem. Phys.* **1954**, *22*, 2013.

(38) Pauling, L. *The Nature of the Chemical Bond;* Cornell University: Ithaca, New York, 1960.

(39) Rothe, E. W.; Neynaber R. H.; Trujillo, S. M. *J. Chem. Phys.* **1965**, *42*, 3310.

(40) Hotop, H. *Radiat. Res.* **1974**, *59*, 379.

(41) Haberland, H.; Lee Y. T.; Siska, P. E. *Adv. Chem. Phys.* **1981**, *45*, 487.

(42) Becke, A. D. *J. Chem. Phys.* **1993**, *98*, 5648.

(43) Frisch, M. J.; Trucks, G. W.; Schlegel, H. B.; Gill, P. M. W.; Johnson, B. G.; Robb, M. A.; Cheeseman J. R.; Keith, T.; Petersson, G. A.; Montgomery, J. A.; Raghavachari, K.; Al-Laham, M. A.; Zakrzewski, V. G.; Ortiz, J. V.; Foresman, J. B.; Cioslowski, J.; Stefanov, B. B.; Nanayakkara, A.; Challacombe, M.; Peng, C. Y.; Ayala, P. Y.; Chen, W.; Wong, M. W.; Andres, J. L.; Replogle, E. S.; Gomperts, R.; Martin, R. L.; Fox, D. J.; Binkley, J. S.; Defrees, D. J.; Baker, J.; Stewart, J. P.; Head-Gordon, M.; Gonzalez, C.; Pople, J. A. *Gaussian 94*, revision D.4 Gaussian, Inc.: Pittsburgh, PA, 1995.

(44) von Niessen, W.; Kraemer, W. P.; Diercksen, G. H. F. *Chem. Phys.* **1979**, *41*, 113.

(45) Ortiz, J. V.; Zakrzewski, V. G. *J. Chem. Phys.* **1996**, *105*, 2762.

(46) (a) Walker, I. C.; Palmer, M. H.; Hopkirk, A. *Chem. Phys.* **1989**, *141*, 365. (b) Palmer, M. H.; Walker, I. C.; Guest, M. F.; Hopkirk, A. *Chem. Phys.* **1990**, *147*, 19. (c) Walker, I. C.; Palmer, M. H. *Chem. Phys.* **1991**, *153*, 169. (d) Palmer, M. H.; Walker, I. C. *Chem. Phys.* **1991**, *157*, 187. (e) Walker, I. C.; Palmer, M. H.; Ballard, C. C. *Chem. Phys.* **1992**, *167*, 61.

(47) Kitao, O.; Nakatsuji, H. *J. Chem. Phys.* **1988**, *88*, 4913.

(48) Al-Joboury, M. I.; Turner, D. W. *J. Chem. Soc.* **1964**, 4434.

(49) Yencha, A. J.; El-Sayed, M. A. *J. Chem. Phys.* **1968**, *48*, 3469.

(50) Dewar, M. J. S.; Worley, S. D. *J. Chem. Phys.* **1969**, *51*, 263.

(51) Turner, D. W.; Baker, C.; Baker, A. D.; Brundle, C. R. *Molecular Photoelectron Spectroscopy*; Wiley-Interscience: London, 1970.

(52) (a) Jonsson, B. O.; Lindholm, E.; Skerbele, A. *Int. J. Mass Spectrom. Ion Phys.* **1969**, *3*, 385. (b) Fridh, C.; Åsbrink, L.; Jonsson, B. O.; Lindholm, E. *Int. J. Mass Spectrom. Ion Phys.* **1972**, *8*, 85. (c) Fridh, C.; Åsbrink, L.; Jonsson, B. O.; Lindholm, E. *Int. J. Mass Spectrom. Ion Phys.* **1972**, *8*, 101. (d) Åsbrink, L.; Fridh, C.; Jonsson, B. O.; Lindholm, E. *Int. J. Mass Spectrom. Ion Phys.* **1972**, *8*, 215. (e) Åsbrink, L.; Fridh, C.; Jonsson, B. O.; Lindholm, E. *Int. J. Mass Spectrom. Ion Phys.* **1972**, *8*, 229.

(53) Gleiter, R.; Heilbronner, E.; Hornung, V. *Helv. Chim. Acta* **1972**, *55*, 255.

(54) Brundle, C. R.; Robin, M. B.; Kuebler, N. A. *J. Am. Chem. Soc.* **1972**, *94*, 1466.

(55) Berg, J. O.; Parker, D. H.; El-Sayed, M. A. *Chem. Phys. Lett.* **1978**, *56*, 411.

(56) Utsunomiya, C.; Kobayashi, T.; Nagakura, S. *Bull. Chem. Soc. Jpn.* **1978**, *51*, 3482.

(57) Reineck, I.; Maripuu, R.; Veenhuizen, H.; Karlsson, L.; Siegbahn, K.; Powar, M. S.; Zu. W. N.; Rong, J. M.; Al-Shamma, S. H. *J. Electron Spectry. and Relat. Phenom.* **1982**, *27*, 15.

(58) Piancastelli, M. N.; Keller, P. R.; Taylor, J. W.; Grimm, F. A.; Carlson, T. A. *J. Am. Chem. Soc.* **1983**, *105*, 4235.

(59) Keller, P. R.; Taylor, J. W.; Carlson, T. A.; Grimm, F. A. *J. Electron Spectrosc. Relat. Phenom.* **1984**, *33*, 333.

(60) Clementi, E. *J. Chem. Phys.* **1967**, *46*, 4731; *47*, 4737.

(61) Petke, J. D.; Whitten, J. W.; Ryan, J. A. *J. Chem. Phys.* **1968**, *48*, 953.

(62) Spanget-Larsen, J. *J. Electron Spectrosc. Relat. Phenom.* **1973**, *2*, 33.

(63) Almlof, J.; Roos, B.; Wahlgren, U.; Johansen, H. *J. Electron Spectrosc. Relat. Phenom.* **1973**, *2*, 51.

(64) Ellis, R. L.; Jaffe, H. H.; Masmanidis, *J. Am. Chem. Soc.* **1974**, *96*, 2623.

(65) Wadt, W. R.; Goddard, W. A., III. *J. Am. Chem. Soc.* **1975**, *97*, 2034.

(66) Wadt, W. R.; Goddard, W. A., III.; Dunning, T. H., Jr. *J. Chem. Phys.* **1976**, *65*, 438.

(67) Ohsaku, M.; Imamura, A.; Hirao, K. *Bull. Chem. Soc. Jpn.* **1978**, *51*, 3443.

(68) Tantardini, G. F.; Simonetta, M. *Int. J. Quantum Chem.* **1981**, *20*, 705.

(69) Moghaddan, M. S.; Bawagan, A. D. O.; Tan, K. H.; von Niessen, W. *Chem. Phys.* **1996**, *207*, 19.

(70) Munakata, T.; Kuchitsu, K.; Harada, Y. *J. Electron Spectrosc. Relat. Phenom.* **1980**, *20*, 235.